Sains Malaysiana 46(11)(2017): 2231-2239
http://dx.doi.org/10.17576/jsm-2017-4611-25

Comparative Analysis of Load Responses and Deformation for Crust Composite Foundation and Pile-supported Embankment

(Perbandingan Analisis Respons Beban dan Kecemaran Asas Komposit Kerak dan Embankmen Disokong Longgokan)

Ying Wang, Yonghui Chen*, Zhenhua Hu, Qiang Feng & Desen Kong

ABSTRACT

Ground improvement using artificial crust composite foundation, consisting of stabilization of soft clay and composite foundation, is an effective technique for the treatment of deep soft soil layers under infrastructure embankments. In this study, the load responses and settlement performance of this improvement technique were investigated using two centrifuge model tests to compare the variations of the vertical deformation, pore water pressure, axial force of the piles and tensile stress at the bottom of the artificial crust in the crust composite foundation with those in pile-supported embankment. The results of centrifuge model tests showed that the load responses and settlement performance of artificial crust composite foundation was different from the pile-supported embankment, which displayed mainly that the final middle settlement of crust composite foundation can be reduced by about 15% compared with those of pile-supported embankment with the same length of pile and construction cost. The deformation of the crust with the characteristics of the plate was found based on the change of the tensile stress. Additionally, the excess pore water pressure in the crust composite foundation was lower owing to the stress diffusion effect of the crust during the loading period and the dissipation rate of excess pore water pressure was slower due to lower permeability of the crust at the same loading period. Eventually, the axial force of the middle piles was reduced. At the same time, the boundary stress was functioned with the crust, the axial force of the side piles was improved. The comparison of measured and calculated results was carried out using the stress reduction ratio, the result shows that the bearing capacity of the subsoil in the crust composite was improved.

Keywords: Artificial crust composite foundation; centrifuge model test; pile-supported embankment; soft clay; stabilization

ABSTRAK

Pembaikan tanah yang menggunakan asas komposit kerak tiruan, terdiri daripada penstabilan tanah liat lembut dan komposit asas, merupakan teknik yang berkesan untuk rawatan tanah lembut lapisan dalam di bawah infrastruktur benteng. Dalam kajian ini, beban tindak balas tindakan dan prestasi penempatan dalam teknik pembaikan ini dikaji menggunakan dua model ujian pengemparan untuk membandingkan perbezaan canggaan menegak, tekanan air liang, daya paksi cerucuk dan tekanan tegangan di bahagian bawah kerak tiruan dalam asas komposit kerak dengan cerucuk disokong benteng. Keputusan ujian model pengemparan menunjukkan bahawa beban tindak balas dan prestasi penempatan asas komposit kerak tiruan adalah berbeza daripada cerucuk disokong benteng, yang memaparkan asas penempatan tengah akhir, asas kerak komposit boleh dikurangkan kira-kira 15% berbanding dengan cerucuk disokong benteng dengan panjang cerucuk serta kos pembinaan yang sama. Canggaan kerak ini dengan ciri plat dijumpai berdasarkan perubahan tekanan tegangan. Di samping itu, tekanan air liang lebihan dalam asas komposit kerak adalah lebih rendah disebabkan kesan penyebaran tekanan kerak pada sepanjang tempoh bebanan dan kadar pelesapan tekanan air liang lebihan adalah lebih perlahan disebabkan oleh kadar resapan kerak yang lebih rendah pada tempoh beban yang sama. Kesimpulannya, daya paksi cerucuk di bahagian telah telah dikurangkan. Pada masa yang sama, tekanan sempadan berfungsi dengan kerak maka daya paksi cerucuk sisi bertambah baik. Perbandingan keputusan yang diukur dan dikira telah dijalankan menggunakan nisbah penurunan tekanan dan keputusan menunjukkan bahawa keupayaan galas tanah bawah dalam komposit kerak adalah bertambah baik.

Kata kunci: *Asas komposit kerak tiruan; benteng disokong cerucuk; model ujian pengemparan; penstabilan; tanah liat lembut*

Introduction

Construction of an embankment on soft clay would induce building settlement and slope stability engineering accident. Accordingly, it is necessary to find an effective solution to treat the soft soil. A combined foundation improvements technology was developed that consisted of in-situ stabilization of the soft clay and composite foundation. The technology was referred to as artificial crust composite foundation (crust composite foundation). The artificial crust formed by *in-situ* stabilization has a higher compressive modulus and cohesion, which replaces the traditional sand cushion and pile cap in pile-supported embankment, reduces the total and differential settlement and improves the global stability of earth structures of high standard roads or high embankments on a deep soft soil layer.

Several studies on the load responses and interaction effects of pile-supported embankment have been reported in the literature. Actually, many researchers have carried out different kinds of model and field tests (Blanc et al. 2014; Chen et al. 2016; Erfen et al. 2017; Fagundes et al. 2017; Zheng et al. 2011) and different analytical methods (Chen et al. 2008; Hewlett & Randolph 1988; Liu et al. 2017; Zhang et al. 2012) to study the pile-supported embankments. More recently, investigators have mainly focused on studying the effect of pile-supported embankments using finite element method (FEM) (Ariyarathne & Liyanapathirana 2015; Huang & Han 2009; Stewart & Filz 2014; Yapage et al. 2014; Zhuang et al. 2012). However, few studies have been conducted on the load responses and interaction effects of the crust composite foundation, even though, the combined foundation improvement technology has been applied. For instance, Jelisic and Leppänen (2003) proposed that the organic soft soil be treated by stabilization combined with the lime piles, but there is no theoretical methods to design. In addition, Ishikura et al. (2016, 2007) reported a new method for predicting the total settlement for the stabilization combined with the floating-type deep mixing soil stabilization method, based on the several loading model tests and field measurements, however, the method was not suitable to calculate the stabilization combined with rigid piles. To the best of our knowledge, the load responses and interaction effects were seldom explicitly considered or systematically investigated in the stabilization combined with rigid piles.

In view of the aforementioned issues, the aimed of this paper was to analyze the difference of the load responses and deformation performance and the reason in the artificial crust composition foundation, not analyzed in previous studies. With this propose, the load responses and deformation in pile-supported embankment and crust composite foundation will be investigated by two centrifuge model tests in the soft foundation, with comparing variations of the vertical deformation, pore water pressure, axial force of the piles and tensile stress at the bottom of the artificial crust in the crust composite foundation with those in pile-supported embankment.

Material and Methods

Centrifuge model tests

The centrifuge model tests reported in this paper were performed at the Geotechnical Centrifuge Facility of Hong Kong University of Science and Technology (Ng 2014; Noor & Ashraf 2017). The purpose of carrying out centrifuge tests was to recreate stress condition which would exist in a full-scale construction (prototype) in a soil model with greatly reduced dimension, by elevating its gravitational acceleration. Since soil properties are governed by effective stress, the behavior of the soil in the centrifuge test would be similar as to that in the field.

Scaling relationships between a centrifuge model and its corresponding prototype are generally derived through dimensional analysis, from the governing equations for a phenomenon, or from the principles of mechanical similarity between a model and a prototype (Garnier et al. 2007; Taylor 1995). The scale factors relevant to this study are summarized in Table 1.

TABLE 1. Scaling factors relevant to centrifuge tests

Physical quantity	Scaling factor (model/prototype)
Gravitational acceleration	n
Length	$1/n$
Area	$1/n^2$
Volume	$1/n^3$
Displacement	$1/n$
Stress	1
Strain	1
Density	1
Time(for consolidation)	$1/n^2$
Flexural rigidity(EI)	$1/n^4$
Bending moment	$1/n^3$

Two centrifuge model tests were conducted to compare the deformation and stress in the pile-supported embankment with those in the crust composition foundation. All centrifuge tests were performed at a centrifugal acceleration of 80 g (g denotes earth gravity) and completed in one flight. A standard model box for centrifuge testing was divided into two equal-sized small boxes by a rigid central divider, as shown in Figure 1(c). One box (i.e. Box A) was used to simulate the deformation and stress in pile-supported embankment, while the other box (i.e. Box B) modeled the crust composite foundation. Each small model box has a plane dimension of 600 × 100 mm (i.e. 48 × 8 m in the prototype) and a depth of 310 mm (i.e. 24.8 m in the prototype). According to Yao et

al. (2004), the boundary effect of the side friction in the centrifugal tests is limited to a distance of approximately 100 mm from the box boundary. In the present study, the distance from the toe of the embankment to the box boundary was 100 mm.

The two models in this centrifuge test were designed based on the same the length of the pile and the approximate cost, as shown in Figure 1(a) and 1(b). In each model box, the same length of the piles was 20 cm (16 m in the prototype) and the height of the embankment was 56.3 mm (4.5 m in the prototype). Meanwhile, the pile spacing was 30 mm (2.4 m in the prototype) and the pile cap had a length of 12.5 mm (1 m in the prototype), a width of 12.5 mm (1m in the prototype) and a thickness of 4.4 mm (0.35 m in the prototype) in pile-supported embankment model box. On the other hand, a pile spacing of 37.5 mm (3.0 m in the prototype) and a crust with the thickness of 21 mm (1.68 m in the prototype) were chosen in the other model box.

A digital camera with a maximum resolution of 2592 × 1944 pixels was mounted at 450 mm at the front of the transparent side wall to capture digital images of the soil at various stages during the in-flight test. The movement of the soil was quantified by processing two subsequent digital images by particle image velocimetry (PIV) analysis coupled with a close-range photogrammetry correction (White et al. 2003).

Besides the measurement of soil and pile movement, pore water pressure transducers and strain gauges were chosen to be used in this study. Pore water pressure transducers were installed underneath each embankment and adjacent to middle pile to confirm the time effect at depths of 31.3 mm (2.5 m in the prototype), 68.8 mm (5.5 m in the prototype), 106.3 mm (8.5 m in the prototype) and 206.25 mm (16.5 m in the prototype) from the surface of the ground. In addition, four strain gauges were installed at the bottom of the crust and five pairs of strain gauges were installed along the pile at the depths of 0.04 L, 0.25 L, 0.5 L, 0.75 L and 0.96 L from the pile top. The piles with strain gauges were placed in the middle and the side of the pile.

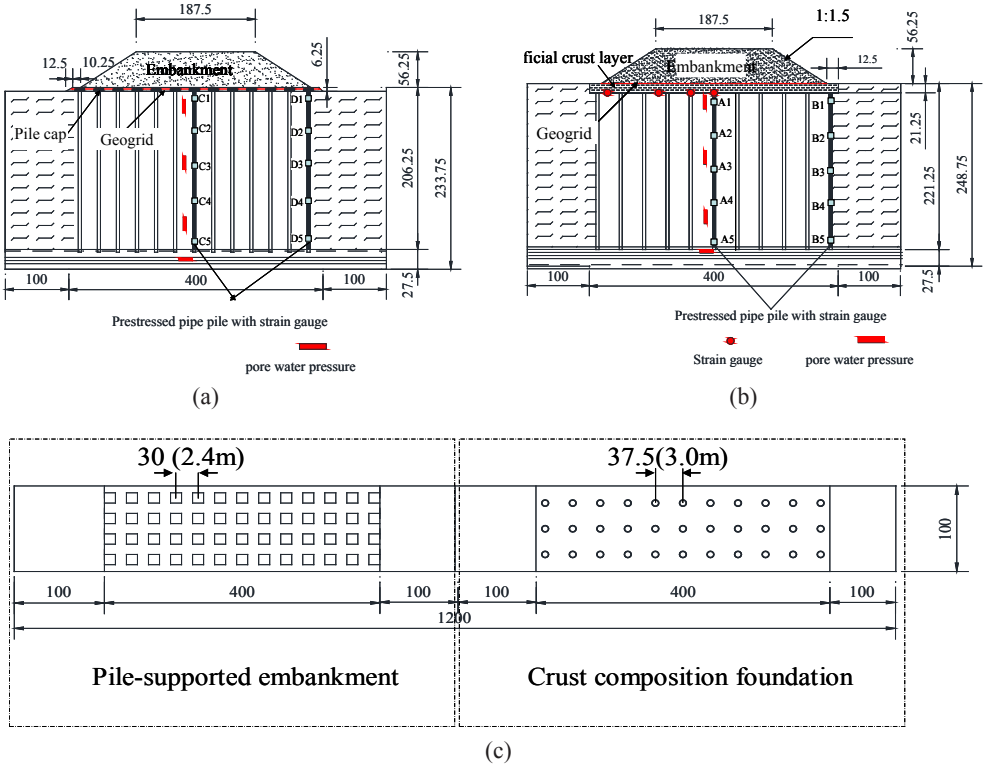

FIGURE 1. Schematic view and arrangement of test model (unit: mm) (a) Pile-supported embankment; (b) crust composite foundation; and (c) A plane diagram

Model material

Crust

Preparation of the crust: The sludge soft soil and 7% of Portland cement were mixed. Water was injected into cement to help it obtain compaction as well as for hydration of the cement (Water-cement ratio is 2:1). The mixture soil was placed in molds, which had a length of 400 mm (32 m in the prototype), a width of 100 mm (8 m in the prototype) and a thickness of 21 mm (1.68 m in the prototype). At the same time, 39.1 × 80 mm triaxial samples were prepared. The molds and triaxial samples were stored in a curing room (maintained at 23±2°C, 95±2% RH), wrapped in a thin damp cloth for 14 days. Before the experiment

started, unconfined compressive strength was measured after the samples was removed from the mold, the average unconfined compressive strength was 550 kPa. As the cracking failure of artificial crust was likely to occur, the tension stress of the crust should be measured in this study. Indeed, the tension stress of the crust was 110 kPa through the axial fracturing test.

TABLE 2. Physical properties of the sludge soft soil

Properties	Value
Water content, ω (%)	45.8
Soil density, ρ (g/cm^3)	1.55
Liquid limit, ω_L (%)	34.4
Plasticity index, I_P (%)	20.2
Specific gravity, G_s	2.72
Void ratio, e	1.59
Modulus of compression, E (MPa)	1.70

PILE

Each pile is modelled by an aluminum tube with an outer diameter and thickness of 5 mm and 0.5 mm, respectively. Since each pile was to be loaded by superstructure, the pile deformation would be governed, which is relevant to the rigidity of the pile. According to the scaling factor for the rigidity (i.e. 1:n^4, Table 1), each model pile is approximately equivalent to a pre-stressed concrete pipe pile with a diameter and thickness of 0.4 m and 6 mm in the prototype. Additionally, the materials of the pile caps were the same as the pile. The pile caps and pile was glued together by using liquid epoxy resin.

SUBSOIL

Experiments were performed using sludge soft soil and silty clay. The sludge soft soil of the third stratum in the centrifuge laboratory of the Hong Kong University of Science and Technology was chosen for the experiment. The physical and mechanical properties of the sludge soft soil was shown in Table 2. The silty clay was used for the bearing stratum, characterized by the maximum dry density, 1.82 g/cm^3 and the optimum water content, 14%.

The centrifuge model foundations adopted in this study are shown in Figure 1. Soil was obtained from the field, air-dried, crushed, and passed through a 2 mm sieve prior to constructing the foundation. Then, the right amount of water was added, stirring evenly. The soil samples were filled to the suitable height of the test box. Simultaneously, the silt clay was prepared with the optimum water content (14%) and a 90% compaction was guaranteed. In addition, the pore water pressure gauges and the piles were also placed in a certain location.

EMBANKMENT

Toyoura sand material were used for the embankment. The special gravity was 2.65, the average particle diameter D50 about 0.17 mm, the maximum void ratio e_{max} 0.977, the minimum void ratio e_{min} 0.597 and the bulk density 1.5 g/cm^3 (Ishihara 1993; Rahman et al. 2014). The main mineral of the Toyoura sand is quartz. Under very high pressure (higher than 4000kPa), the sand will be crushed. Therefore, it did not need to be taken into account that the characteristics of this sand were changed due to the sand particle crushing.

The specimens of the embankment were prepared by the raining method using a sand diffuser system that consisted of a sand hopper and a parallel manipulator. The raining method was performed twice through the height of the embankment, as shown in Figure 2. In order to simulate the uniform load, the sanding speed of 5.0 g/s in the first loading and the speed of 2.83 g/s in the second loading.

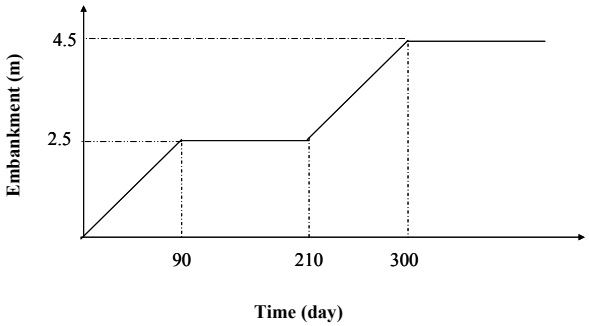

FIGURE 2. Load versus time

GEOGRID

Geogrid when used as a reinforcement can resist the spreading of the embankment and the lateral displacement of the foundation and thus contributes to the stability of the embankment. A geogrid mobilizes its tensile resistance mainly by generating passive resistance to the soil particles confined between its apertures (Sharma & Bolton 1996). The use of a scaled-down geogrid for model reinforcement was well discussed by Viswanadham and Mahajan (2004). Two scaling relationships were deduced for a model geogrid considering two basic requirements: scaling of the tensile stiffness and scaling of the bonding strength, i.e.

$$\frac{J_m}{J_p} = \frac{1}{N} \quad , \tag{1}$$

$$\frac{f_m}{f_p} = 1 \, , \tag{2}$$

where J is the secant modulus of the geogrid, which is equal to its Young's modulus Er multiplied by its cross-section area Ar; f is the coefficient of interface friction between the soil and geogrid; subscripts m; and p stand for model and prototype, respectively.

The design requirements of the geogrid in practical engineering are as follows: Geogrid should adopt two-way geogrid; should be no greater than the breaking elongation of 3% and not less than a tensile strength of 80 kN/m.

A plastic window screen was used to simulate the prototype geogrid in the present study. The tension-strain curves of the model geogrid obtained by testing 50 mm wide and 100 mm long strips in a tensile testing machine are shown in Figure 3. The model geogrid has an average secant modulus of 40 kN/m and a tensile strength of 1.0 kN/m at 3% axial strain, equivalent to a secant modulus of 3200 kN/m and a tensile strength of 80 kN/m for a prototype geogrid at the same strain with an acceleration of 80 g. Compared with the tensile test results, the plastic window screen can meet the design requirements.

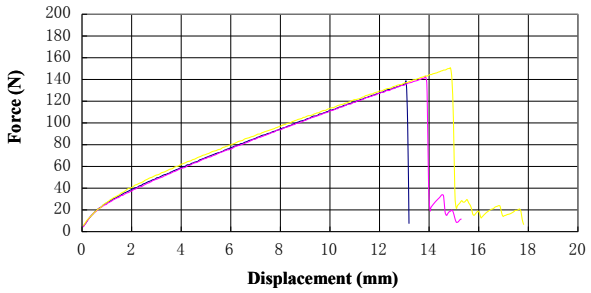

FIGURE 3. longitudinal tensile test of plastic window screen

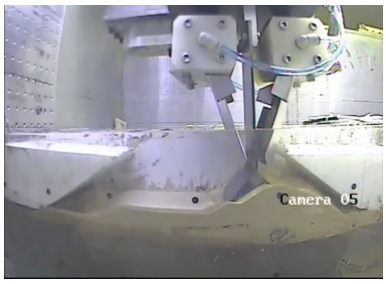

(a)

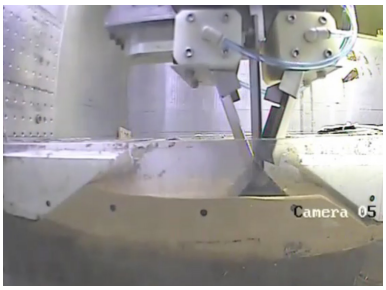

(b)

FIGURE 4. Embankment prepared
(a) sprinkling sand and (b) leveling with the parallel manipulator

Centrifuge modeling procedure

A thin film of silicone grease was smeared onto the inside vertical surfaces of the strongbox to reduce the friction. Before running the centrifuge, the markers in the model were recorded by the camera, therefore, as to analyze the ground subsidence at different depths.

The subsoil was placed in 9 layers in 30 mm lifts. Then crust, geogrid, piles and pore pressure transducers were installed at various locations in the subsoil, as shown in Figure 1. In order to reach a stress level and degree of consolidation in the model foundation like that in the prototype, the model was subjected to an acceleration of 80 g until the consolidation of the foundation was achieved.

Eventually, the embankment started to sprinkle sand by the raining method using a sand diffuser system. The specific process: A trapezoidal plastic model of the embankment was made. The two-stage construction of the embankment was simulated by the raining methods, as shown in Figure 4. In the first construction stage, a sand diffuser system moved to the model border, the sand hopper starts to sprinkle sand and the parallel manipulator also starts to move back until the sand content of the first stage is finished. At the end, the sand surface was leveled with the parallel manipulator.

The second construction stage was the same as the first stage. In the first construction stage, the embankment of 31.25 mm (2.5 m in the prototype scale) was controlled in 20.25 min and then was running for 27 min at the same thickness. Similarly, in the second construction stage, the embankment of 25 mm (2 m in the prototype scale) was controlled in 20.25 min.

Results

In this paper, interpretation of the results is only focused on the responses of the ground and pile due to the construction of the embankment. All results are presented in the prototype scale, unless stated otherwise. In the figures, the crust was replaced as the crust composite foundation and cushion was also replaced as pile-supported embankment.

Surface settlement of foundation

The settlement-time-load curves of pile-supported embankment and crust composite foundation obtained from the centrifuge tests performed at the middle and embankment toe location are shown in Figure 5. These curves (Figure 5) show that the total settlement of pile-supported embankment was higher than that of the crust composite foundation at the same time. The settlement in the middle of the cushion and crust composite foundations measured at 300 day, corresponding to the end of the construction, were 20.6 and 18.0 cm, respectively and at the 2000 day, assumed to be close to the end of the settlement, the settlement in the middle of the cushion and crust composite foundations were 33.6 and 28.4 cm.

The post-construction settlements of the cushion and crust composite foundations were 13.0 and 10.4 cm in the prototype, both of which can meet the engineering requirements. This data shows that the total and post-construction settlements were reduced when using the crust composite foundation and the eventual settlement in the middle of the crust composite foundation can reduced by about 15% compared with that in pile-supported embankment.

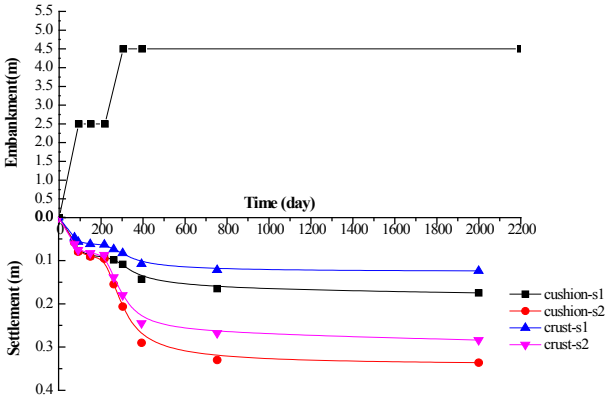

FIGURE 5. Settlement versus time

A calculated method was proposed by Chen et al. (2008) to study pile-supported embankment. Using this method, the settlement of pile-supported embankment is 33.4 cm, which is agreed well with the experimental settlement. Based on the calculated method, the settlement of pile-supported embankment is 33.1 cm with the same treated depth. With the same treated depth and the spacing of the piles, the settlement of pile-supported embankment is 46.0 cm, increased by about 39% compared with the crust composite foundation and the length of the piles increased by 10%, the settlement only reduced by about 0.9% in pile-supported embankment, which shows that the difference was negligible owing to the changing of the length of the piles. Hence, the two the centrifuge tests can be compared with the same length of piles.

The settlement of embankment toe in two cases at 2000 day were 17.5 and 12.4 cm in the prototype, respectively, and at the 300 day, the settlement in the embankment toe of two cases were 10.9 cm and 8.3 cm in the prototype, respectively. This data show that the settlements of the embankment toe were also reduced in the crust settlement of the foundation.

TENSION STRESS OF THE CRUST

The cracking damage and pricking destruction of the crust in the crust composite foundation are the events most likely to occur. To study the cracking destruction of the crust, strain gauges were posted in the zone prone to cracking damage. Additionally, as the artificial crust stress change with time, the time and location of the maximum tensile stress should be known. Tensile stress-time curves are shown in Figure 6, which shows that the largest tensile stress occurred in the middle of the crust. Moreover, the characteristics of a similar plate were taken to rely on the tensile stress changing, and the pricking destruction of the pile occurred in the middle crust. The data presented in Figure 6 also shows that the tensile stress increases with the load, but the tensile stress decreased at equal loading because of the consolidation of the subsoil, Accordingly, the maximum tensile stress occurred at the end of the construction. Thus, in conclusion, the cracking damage of the crust occurred during the loading period. The average compressive strength of the crust was 550 kPa and the limit tensile stress of 110 kPa was measured, the tensile strength of artificial crust was equal to 20% of the compressive strength, q_u . The tensile stress of the model did not reach the limit tensile stress. Thus, the integrity of the artificial crust was ensured.

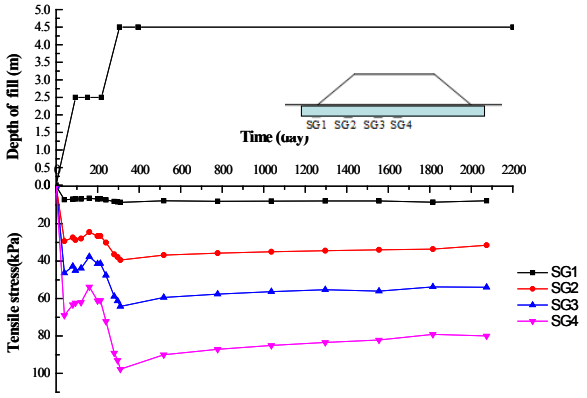

FIGURE 6. Tension stress of the crust

EXCESS PORE WATER PRESSURE

In the study of the stress transfer and the consolidation rate of the subsoil, the most direct performance is the excess pore water pressure. The excess pore water pressure-time-load curves are plotted in Figure 7. The maximum excess pore pressure near the surface of the ground was approximately 8.8 kPa based on crust composition foundation and 13.0 kPa based on cushion composition foundation, this value was recorded at the end of the second phase of construction. The excess pore water pressure in pile-supported embankment is higher during the loading period and the dissipation rate of the excess pore water pressure is faster at the same loading period compared with the crust composite foundation. The maximum excess pore pressure developed in the clay was not very high because a large portion of the embankment load was transferred to the piles as a result of soil arching within fill layers, shear stress developing in the piles-soil interface and dissipation of generated excess pore pressures during the construction (Ishikura et al. 2016; Yapage et al. 2014).

The excess pore water pressure near the surface of pile-supported embankment and crust composite foundation measured at the first construction stage were 12.0 and 7.3 kPa, respectively and at the first equal loading stage, the excess pore water pressure of two cases were 2.7 and 6.3 kPa, respectively. For the same time, 77.5% consolidation settlement is achieved in pile-supported embankment, but only 14% consolidation settlement is achieved in the crust composite foundation. The different responses of the excess pore water pressure can be explained based on the crust. The foundation stress in the crust composition foundation can be spread because of the crust with the properties of plate and was reduced due to the conflict between the crust and the subsoil, at the same time, the permeability of the crust was lower, thus the consolidation rate became slower.

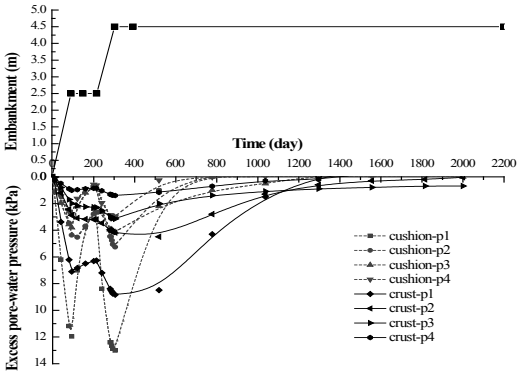

FIGURE 7. Excess pore water pressure versus time

AXIAL FORCE OF THE PILE

In order to investigate the load-transfer mechanism, the axial force transfer curves of two cases were obtained and are plotted in Figure 8. During consolidation, the axial force in piles increased both two cases because of the transfer of more loads to the piles (Huang & Han 2009). The results for the middle pile in pile-supported embankment indicate that the axial force transfer is larger than that in the crust composite foundation. However, the results for the side pile in pile-supported embankment indicate that the axial force transfer is smaller than that in the crust composite foundation. This can be explained by various factors, including that: The redistribution of foundation stress with the properties of the crust, the fully functioning bearing capacity of the side section and the conflict between the crust and the subsoil (Ishikura et al. 2016).

As shown from Figure 8(b), The axial force of the side pile in the crust composite foundation was smaller at 4~8 m at the low embankment, which clearly shows the deformation difference value between piles and subsoil is larger, this also shows that the stress at the boundary was larger because of the crust with the properties of plate.

The structure of the crust composite foundation was similar as that of pile-supported embankment. Sand-gravel cushion and pile cap was replaced by the artificial crust. Several design methods of pile-supported embankment have been developed. Two method was proposed to calculate stress reduction ratio (S3D), one of them is Hewlett and Randolph's arching model (referred to as the H&R method in the remainder of the paper) incorporated in the British Standards BS8006 (BS 2010). The H&R method (Fagundes et al. 2017; Zhuang et al. 2012) regards the arching effect as a single hemispherical dome transferring loads to the pile. The other is the BS8006 with some modification by van Eekelen et al. (2011). In pile-supported embankment, the S3D, at the embankment of 4.5 m, calculated by the above two methods is 67.6% (the angle of friction of the embankment is 30°) and 32.5%, respectively, while the measured result is 48.5%. The measured result was close to the average calculated result. On the other hand, the S3D for the crust composite foundation calculated by the above two methods is 83.7% (the angle of friction of the crust is 20°) and 57.4%, respectively and the measured result was 72.3%. The measured result was close to the calculated result by the H&R method. Such a large difference indicates that the bearing capacity of the subsoil in the crust composite was improved.

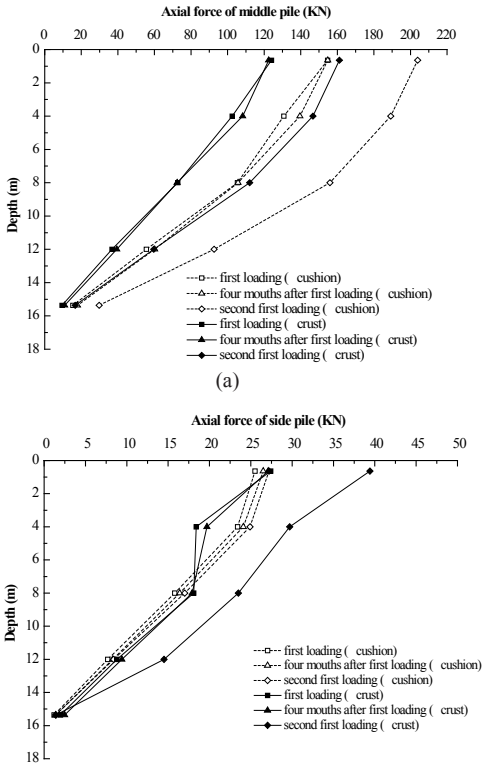

FIGURE 8. Axial force of the piles: (a) middle pile and (b) side pile

Discussion

Generally, artificial crust composite foundation consisting of stabilization of soft clay and composite foundation, is an effective technique for the treatment of deep soft soil layers under infrastructure embankments. Compared with the structure of pile-supported embankment, the main different section is that the stabilized curst instead of the sand-gravel cushion and pile cap. In the artificial crust composite foundation, the primary function of a stabilized crust is to transfer stresses from the embankment over the soft clay layer to individual piles and to reduce the differences in settlement owing to the higher modulus of compression of the crust. At the same time, the results of the centrifuge tests in the artificial crust composition foundation implied that foundation stress is diffused and bearing capacity of the side section is fully functioned due to the effect of crust. Therefore, the settlement performance and the load responds is different from the pile-supported embankment. In summary, the analytical methods of pile-supported embankment are not applied to analyze the artificial crust composition foundation, the function of the crust should be fully considered in the future analytical methods.

Conclusion

Two centrifuge model tests (completed in a single flight) were conducted to study the load responses and deformation in the crust composite foundation compared with pile-supported embankment. In the two simulated cases, the two typical scenarios were modeled to compare the load responses and deformation in the two cases. In addition, the deformation characteristics of the crust in the crust composite foundation were also investigated. Based on the investigations, the following conclusions can be drawn:

By comparing the deformation in the two simulated cases, it was found that the final middle settlement of the crust composite foundation can be reduced by about 15% compared with those of the composite cushion foundation.

In response to the two-distinct excess pore water pressure mechanisms, the excess pore water pressure in pile-supported embankment is higher during the loading period and the dissipation rate of the excess pore water pressure is faster at the same loading period compared with the crust composite foundation. The explanation for this event is that the stress can be spread and reduced due to the crust with the properties of plate. Thus, the consolidation rate became slower based on the low permeability of the crust.

By comparing the axial force of the piles in the two simulated cases, the axial force of the middle pile in pile-supported embankment are larger than that in the crust composite foundation. However, the axial force of side pile in pile-supported embankment is smaller than that in the crust composite foundation. This can be explained by the following observations: the redistribution of foundation stress by the crust with the properties of plate, the fully functioning bearing capacity of the side section and the conflict between the crust and the subsoil.

The tensile stress-time curves show that the largest tensile stress occurred in the middle of the crust and the characteristics of a similar plate was taken to depend on the tensile stress changing, as well as on the maximum tensile stress occurring at the end of the construction. In conclusion, cracking damage of the crust occurred during the loading period.

Acknowledgements

This research was financially supported by the National Natural Science Foundation of China (No. 41372288), Natural Science Foundation of Shandong Province (ZR2016JL018, ZR2017BD037) and the Scientific Research Foundation of Shandong University of Science and Technology for Recruited Talent (2017RCJJ055).

References

Ariyarathne, P. & Liyanapathirana, D.S. 2015. Review of existing design methods for geosynthetic-reinforced pile-supported embankments. *Soils and Foundations* 55(1): 17-34.

Blanc, M., Thorel, L., Girout, R. & Almeida, M. 2014. Geosynthetic reinforcement of a granular load transfer platform above rigid inclusions: Comparison between centrifuge testing and analytical modelling. *Geosynthetics International* 21(1): 37-52.

BS 8006. 2010. *Code of Practice for Strengthened/ Reinforced Soils and Other Fills*. British Standard Institution, UK.

Chen, R.P., Wang, Y.W., Ye, X.W., Bian, X.C. & Dong, X.P. 2016. Tensile force of geogrids embedded in pile-supported reinforced embankment: A full-scale experimental study. *Geotextiles & Geomembranes* 44(2): 157-169.

Chen, R.P., Chen, Y.M., Han, J. & Xu, Z.Z. 2008. A theoretical solution for pile-supported embankments on soft soils under one-dimensional compression. *Canadian Geotechnical Journal* 45: 611-623.

Erfen, H.F.W.S., Asis, J., Abdullah, M., Musta, B., Tahir, S., Pungut, H. & Mohd Husin, M.A.Y. 2017. Geochemical characterization of sediments around Nukakatan Valley, Tambunan, Sabah. *Geological Behavior* 1(1): 13-15.

Fagundes, D.F., Almeida, M.S.S., Thorel, L. & Blanc, M. 2017. Load transfer mechanism and deformation of reinforced piled embankments. *Geotextiles & Geomembranes* 45(2): 1-10.

Garnier, J., Gaudin, C. & Springman, S.M. 2007. Catalogue of scaling laws and similitude questions in geotechnical centrifuge modelling. *International Journal of Physical Modelling in Geotechnics* 7(3): 1-23.

Hewlett, W.J. & Randolph, M.F. 1988. Analysis of piled embankments. *Ground Engineering* 21(3): 12-18.

Huang, J. & Han, J. 2009. 3D coupled mechanical and hydraulic modeling of a geosynthetic-reinforced deep mixed column-supported embankment. *J. Geotextile Geomembr.* 27(4): 272-280.

Ishihara, K. 1993. Liquefaction and flow failure during earthquakes. *Géotechnique* 43(3): 351-451.

Ishikura, R., Yasufuku, N. & Brown, M.J. 2016. An estimation method for predicting final consolidation settlement of ground improved by floating soil cement columns. *Soils & Foundations* 56(2): 213-227.

Ishikura, R., Ochiai, H., Yasufuku, N. & Omine, K. 2007. Estimation of the settlement of improved ground with floating-type cement-treated columns. *Proceedings of the 4th International Conference on Soft Soil Engineering*, Vancouver. pp. 625-635.

Jelisic, N. & Leppänen, M. 2003. Mass stabilization of organic soils and soft clay. *Proceedings of the 3th International Conference on Grouting and Ground Treatment*, New Orleans, Louisiana. pp. 552-561.

Liu, W., Qu, S., Zhang, H. & Nie, Z. 2017. An integrated method for analyzing load transfer in geosynthetic-reinforced and pile-supported embankment. *KSCE Journal of Civil Engineering* 21(3): 687-702.

Ng, C.W.W. 2014. The state-of-the-art centrifuge modelling of geotechnical problems at hkust. *Journal of Zhejiang University-Science A* 15(1): 1-21.

Noor, M.J. & Ashraf, M.A. 2017. Accumulation and tolerance of radiocesium in plants and its impact on the environment. *Environment Ecosystem Science* 1(1): 13-16.

Rahman, M.M., Abdullah, R.B., Wan Khadijah, W.E., Nakagawa, T. & Akashi, R. 2014. Feed intake and growth performance of goats offered Napier grass (*Pennisetum purpureum*) supplemented with concentrate pellet and soya waste. *Sains Malaysiana* 43(7): 967-971.

Sharma, J.S. & Bolton, M.D. 1996. Centrifuge modelling of an embankment on soft clay reinforced with a geogrid. *Geotextiles & Geomembranes* 14(1): 1-17.

Stewart, M.E. & Filz, G.M. 2014. Influence of clay compressibility on geosynthetic loads in bridging layers for column-supported embankments. *Geo-frontiers Congress* 156(130): 1-14.

Taylor, R.N. 1995. *Geotechnical Centrifuge Technology*. London: Blackie Academic and Professional.

van Eekelen, S.J.M., Bezuijen, A. & van Tol, A.F. 2011. Analysis and modification of the British Standard BS8006 for the design of piled embankments. *Geotextiles & Geomembranes* 29(3): 345-359.

Viswanadham, B.V.S. & Mahajan, R. 2004. Modeling of geotextile reinforced highway slopes in a geotechnical centrifuge. In *Geotechnical Engineering for Transportation Project,* edited by Yegian, M.K. & Kavazanjian, E. *Proceedings of Geo-Trans.* pp.637-646.

White, D.J., Take, W.A. & Bolton, M.D. 2003. Soil deformation measurement using particle image velocimetry (PIV) and photogrammetry. *Géotechnique* 53(7): 619-631.

Yao, M.Y., Zhou, S.H. & Li, Y.C. 2004. Boundary effect analysis of centrifuge test. *Chin Q Mech.* 25(2): 291-296.

Yapage, N.N.S., Liyanapathirana, D.S., Kelly, R.B., Poulos, H.G. & Leo, C.J. 2014. Numerical modeling of an embankment over soft ground improved with deep cement mixed columns: Case history. *Journal of Geotechnical & Geoenvironmental Engineering* 140(11): 04014062.

Zhang, L., Zhao, M., Hu, Y., Zhao, H. & Chen, B. 2012. Semi-analytical solutions for geosynthetic-reinforced and pile-supported embankment. *Computers & Geotechnics* 44(44): 167-175.

Zheng, G., Jiang, Y., Han, J. & Liu, Y.F. 2011. Performance of cement-fly ash-gravel pile-supported high-speed railway embankments over soft marine clay. *Marine Georesources & Geotechnology* 29(2): 145-161.

Zhuang, Y., Ellis, E. &Yu, H.S. 2012. Three-dimensional finite-element analysis of arching in a piled embankment. *Géotechnique* 62(12): 1127-1131.

Ying Wang, Zhenhua Hu, Qiang Feng & Desen Kong
Shandong Provincial Key Laboratory of Civil Engineering Disaster Prevention and Mitigation
Shandong University of Science and Technology
Qingdao 266590
China

Yonghui Chen*
Geotechnical Research Institute
Hohai University, Nanjing 210098
China

*Corresponding author; email: jiang101215@163.com

Received: 8 January 2017
Accepted: 8 June 2017